SPE SAS-1047

A New Approach to Determine Filter Cake Properties of Water-Based Drilling Fluids

S.M. Elkatatny, M.A. Mahmoud, and H.A. Nasr-El-Din, Texas A&M University, All SPE members.

This paper was prepared for presentation at the 2011 SPE Saudi Arabia Section Technical Symposium and Exhibition held in AlKhobar, Saudi Arabia, 15–18 May 2011.

Abstract

Previous studies indicated that the filter cake was heterogeneous and contained two layers with different properties such as thickness, porosity, and permeability. The difference in properties will affect the filtration process and the filter cake buildup for each layer. Previous models of filter cake buildup assumed that the filter cake was homogenous and contained one layer, which undergoes compression followed by buildup.

The objective of this study is to measure the thickness of the two layers of the filter cake and its effect on the filtration process by using a new approach. Our objective also is to develop a valid method to determine local filtration properties, porosity and specific resistance, for each layer in the filter cake. A HPHT filter press was used to perform the filtration process under static conditions (225 ^{o}F and 300 psi). CT (computed tomography) scanner was used to measure the thickness and porosity of the filter cake.

The results obtained from the CT scan showed that there was an inflection time at 7.5 min of filtration at which the process changed from the compression to buildup. Compression region before 7.5 min, in which the thickness of the external and internal layer decreased and there is a great change in the average porosity in both layers. Buildup region after 7.5 min, in which the thickness of the internal layer increased from 0.03 to 0.07 in. and the average porosity decreased from 35 to 15%. The thickness of the external layer also increased from 0.04 to 0.09 in. and the average porosity decreased from 25 to almost 0.0% due to poor sorting in this layer, which prevented more filtration thereof. The new approach better explained the change in thickness and porosity of each layer of the filter cake with time.

Introduction

The filtration properties are an important characteristic of all drilling fluid. The filtrate invation into the formation can substantially reduce the permeability of the near wellbore region by a number of different mechanisms: particle plugging, clay swelling, and water blocking. In addition, the nature and the thickness of the filter cake deposited on the formation face will increase the potential for differential pressure sticking.

Arthurn (1988) discussed the fluid flow through the filter cake. He mentioned that as the suspended solids are deposited during the cake filtration, liquid flow, as a result of the hydraulic pressure gradient through the filter cake. A drag force is therefore exerted on the solid particles and is cumulative as liquid flows through the filter medium. He also stated that, the compressible filter cake exhibits non-linear permeability and porosity profiles, with a maximum porosity at the cake surface, the drag force equal to zero, and minimum at the filter medium surface.

Jiao and Sharma (1994) illustrated that the cake growth rate gradually decreased until an equilibrium filtration rate is attained at which no particles small enough to be deposited are available in the suspension.

Khatib (1994) stated that the cake porosity is not constant and varies with the applied pressure particularly for compressible particles and the filter cake characteristics of the solids can be defined by developing empirical permeability-porosity correlations.

Fathi and Theliander (1995) developed a method to determine the local filtration properties such as specific filtration resistance and porosity. The buildup of the filter cake was simulated by layer by layer model as shown by Theliander and Fathi (1996). They found that change in pressure during the buildup was close to the measured one.

The reduction in local permeability of the filter cake results from two factors: cake consolidation and cake clogging (Tien et al. 1997). Cake consolidation arises from the compressive stress within the cake while cake clogging is caused by the retention of fine particle. The amount of the fines involved may be small but its effect on permeability can be substantial.

A relatively simple approximate model has been developed by Tiller et al. (1999) to describe the behavior of compactible cakes deposited under constant applied pressure. Zinati et al. (2009) developed simple model that can predict the cake thickness and velocity profiles in radial geometry for a suspension containing mono-sized particles. They showed that simplifying assumptions may lead to errors in predicting the cake profiles.

The objectives of this paper are to obtain: (1) the filter cake properties such as thickness, porosity, and (2) permeability of the two layers by using a computed tomography (CT) scanner.

Experimental Studies

Materials

Water-based polymer drilling fluid was used in the experiments, which contained calcium carbonate (50 microns) as a weighting material and bentonite was used as a viscosifier, the composition of the drilling fluid is given in **Table 1**.

Ceramic disks (10 µm) of permeability 775 md were used to stimulate the formation for filtration process at a desirable temperature and pressure.

Preparation of Drilling Fluid

The drilling fluid was prepared by mixing 350 g deionized water (base fluid) with 18 g bentonite, which was used as a filtration control agent for 20 minutes. 0.25 g of sodium carboxy methyl cellulose, which was used as a HPHT filtrate control agent was added and mixed for 5 minutes. 4.0 g of highly oxidized leonardite, which was used as a thinner was added with 0.6 g of caustic soda, which was used as an alkalinity agent, and they were mixed for 5 minutes. 28 g of calcium carbonate, which was used as a weighting and bridging material was added and mixed for 10 minutes. Finally, 27 g of altered calcium montmorillonite clay, which was used as a simulated fluid was added and mixed for 5 minutes.

Properties of the Drilling Fluid

Table 2 summarizes the properties of the drilling fluid. The mud properties were measured by using mud balance and Fann 35 viscometer. The results obtained were 69 pcf for density, 12 cp for a plastic viscosity measured at 120 ^oF, and 8 lb/100 ft^2 for a yield point.

HPHT Filtration

Static HTHP filtration tests were performed using a standard HPHT filter. The cell was placed in a heating jacket and the system was heated to the desirable temperature (225 ^oF). The applied pressure was 300 psi differential pressure.

The filtrate volume was measured at 1, 3, 5, 10, 15, 20, 25, and 30 min and the filter cakes were scanned by using CT scan. The density of filtrate was measured using a high temperature density meter (DMA 4100) at different temperatures as shown in **Fig. 1** and the filtrate viscosity was 0.2 cp at 225 ^oF as shown in **Fig. 2** , measured using a capillary tube viscometer (Ubbelhold type).

Results and Discussion

Porosity Determination

The filter cake was scanned twice in wet and dry conditions for each time of filtration as shown in **Fig. 3.** It was shown that the filter cake contained two layers with different thickness with time. The ceramic disk was scanned before the experiment in wet and dry conditions to determine its initial porosity. The CTN (CT number) for wet conditions was 1550 and for dry conditions was 1180.

From the CT scanner results, the porosity of each layer and the porosity of the ceramic disk can be obtained using Eq. 1.

$$\emptyset = \frac{CT_{wet}-CT_{dry}}{CT_{water}-CT_{air}}, \qquad (1)$$

where

CT_{wet} = CTN of the slice with core saturated with water
CT_{dry} = CTN of the slice when the core is dry
CT_{water} = CTN of water
CT_{air} = CTN of air.

Table 3 summarizes the calculation of porosity for both layers and for the filter medium. It was shown that there was a large variation in the porosity of each layer before 7.5 min (compression time) and there is a specific trend of the average porosity of each layer after 7.5 min (Buildup time).

Fig. 4 illustrates the average porosity of the internal layers at 1 min (ε_0) was 50%, the time before compression start, and this value decreased to 17% at 3 mins as a result of drag force, which acting on the particle due to the cross flow as discussed by Al-abduwani et al. (2005), and Zinati et al. (2009). The average porosity of the internal layer then increased to 45% as more precipitation occurred. After 7.5 min, the average porosity of the internal layers started to decrease from 35 to 15 vol.%

as the filter cake buildup. During this period there were mainly two forces acting on the internal layer, the drag force and the effect of the external layer, which act as a piston on the internal layer.

The average porosity of the external layer was 85% when no compression occurred (ε_0) as shown in **Fig. 4**. In the compression region before 7.5 min, there was a large decrease in average porosity to 5% due to the presence of a high drag force and then increased to 55% as more precipitation occurred. After 7.5 min the build up region, there was a normal trend of the average porosity, which decreases from 22 to 0.0 % as a result of poor sorting in the external layers.

The value of the average porosity of the internal and external layer at time of no compression (ε_0) was comparable with the value given by Fathi and Theliander (1995).

The porosity of the filter disk was calculated using Eq. 1. Before the filtration process porosity was found to be 37% and after the filtration process porosity was in the range from 20 to 25%. The change in porosity of the filter disk indicated variation in its permeability, which should be considered when calculating of the filter cake permeability

Calculation of Filter Cake Thickness

Table 4 summarizes the thickness calculations for the internal and external layers. **Fig. 5** shows that the both layers passed with two regions during the filtration process. The thickness of the internal layer decreased from 0.07 to 0.03 in. in the compression region, and the thickness of the external layer also decreased from 0.04 to 0.02 in. The thickness of the internal layer was greater than the thickness of the external layers as a result of the precipitation of large particles in this region under static condition, as shown by Jio and Sharma (1994), and Civan (1998).

In the buildup region, which appeared after 7.5 min, as shown in **Fig. 5**, the thickness of the internal layer started to increase from 0.035 to 0.07 in. at 30 min. Also, the thickness of the external layer increased from 0.02 to 0.09 in. at 30 min, the end time of filtration process.

The thickness of the internal layer was less than the thickness of the external layer in the buildup region, which reflected the effect of the change in porosity of the external layer in this region. As the porosity of the external layer decreased no more particles could move through the filter cake and hence poor sorting occurred and as a result the thickness of the external layer increased.

Permeability Determination

Depending on the porosity of the external and internal layers, which obtained from the CT scanner, permeability of both layers can be calculated from an empirical correlation Eq. 2 developed by Khatib (1994). **Table 5** summarizes the calculation of this method.

$$k_c = 112.7 * e^{-8.8(1-\emptyset_c)}, \quad \text{(2)}$$

where

k_c = permeability of the mud cake, md

ϕ_c = porosity of the filter cake, volume fraction

As porosity decreased with filtration time, average permeability of the filter cake and permeability of the external and internal layers decreased with time as shown in Fig. 6. This method simulated what occurred in the filtration operation. No filtration occurred after 30 min which result from the decrease of permeability of the external layer till reached a zero value at this time. This method overestimated the values of the permeability of the filter cake and gave higher values as compared with the values given by Elkatatny et al. (2011).

The change in permeability of filter media can be obtained from Eq. 3 developed by Lambert (1981). From CT scan experiments, initial porosity was 37% and final porosity was found to be 20-25%.

$$\frac{k_{final}}{k_{initial}} = M\left(\frac{\emptyset_f}{\emptyset_i}\right)^n, \quad \text{(3)}$$

where

k_{final} = permeability of ceramic disk after filtration process, md

ϕ_f = final porosity of ceramic disk after filtration process, volume fraction

k_{intial} = initial permeability of ceramic disk, md

ϕ_i = initial porosity of ceramic disk, volume fraction

$\Delta\phi_{max}$ = 0.08, M = 1, and n = 3.

Table 6 shows that the permeability of the filter disk reduced by 85% as the porosity reduced to 20%. The reduction of the

filtrate rate with time was shown in **Fig. 7**. Using the flow rate, the average permeability of the filter cake can be obtained by using Li et al. (2005) method. **Table 7** summarizes the calculations based on Eqs. 4-6.

$$q = k_m \frac{\Delta P_m}{\mu L_m} \text{,} \quad \text{(4)}$$

$$\Delta P_t = \Delta P_m + \Delta P_c \text{,} \quad \text{(5)}$$

$$q = k_c \frac{\Delta P_c}{\mu L_c} \text{,} \quad \text{(6)}$$

where

q = filtrate rate, m^3/m^2-s
K_m = filter medium permeability, m^2
K_c = filter cake permeability, m^2
L_m = thickness of filter medium, m
L_c = thickness of filter cake, m
μ = filtrated fluid viscosity, Pa.s
ΔP_m = pressure drop across the filter medium, Pa
ΔP_c = pressure drop across the filter cake, Pa
ΔP_t = total pressure drop, Pa

Fig. 8 shows that the average filter cake permeability was 1.17 µd at initial period of filtration, decreased to nearly 0.4 µd from 5 to 25 min and reduced to zero at the end of filtration. Depending on the porosity obtained from the CT scanner for each layer, the permeability ratio of the external and internal layer can be obtained using Khatib (1994) method, Eq. 7.

$$\frac{k_1}{k_2} = e^{-8.8(\emptyset_2 - \emptyset_1)} \text{,} \quad \text{(7)}$$

where

k_1 = permeability of the external layer, md
k_2 = permeability of the internal layer, md
ϕ_1 = porosity of the external layer, vol. fraction
ϕ_2 = porosity of the internal layer, vol. fraction

The permeability of each layer can be determined using Eq. 8:

$$k_{ave} = \frac{h_t k_1 k_2}{h_1 k_2 - h_2 k_1} \text{,} \quad \text{(8)}$$

where

k_{ave} = average filter cake permeability, md
h_1 = thickness of the external layer, in.
h_2 = thickness of the internal layer, in.

Table 8 summarizes the calculations of the permeability ration, the permeability of each layer, and the pressure drop in each layer. In the compression region, the thickness of the internal layer was higher than the thickness of the external layers, so the pressure drop due to the drag force was higher in the internal layer as compared with the external layer. While in the build up region, due to the reduction of porosity and increase in the thickness of the external layer, the pressure drop in the external layer was higher as compared with the internal layer as shown in **Fig. 9**.

Fig. 10 shows that the permeability of internal layers was smaller than the permeability of the external layer at the first time of filtration due to the effect of the drag force and most of pressure drop occurred in the internal layer. With more filtration, the permeability of the external layer decreased to 0.25 µd and finally decreased to zero at the end of filtration due to the continuous reduction in porosity until reaching a zero value after 30 min of filtration. While the permeability of the internal layer, in the build up region, increased to 1.5 µd and became constant to the end on filtration, as shown in **Fig. 10**.

Conclusions

Filter cake generated by water-based drilling fluids was eaxamined for different time using CT scanner. Porosity was determined from CT scanner, which was used to determine permeability of filter cake. Various models were examined.

Based on experimental results, the following conclusions can be drawn:

1. During the filtration operation there was an inflection time at 7.5 min at which the process changed from compression to buildup.
2. The CT scan provided a good method to obtain the change in the thickness and porosity of both layers of the filter cake. Also, it provided the change in filter media properties, which should be considered in the calculation of the filter cake permeability.
3. The empirical correlation given by Khatib (1994) provided a good simulation of the change in permeability of both layers depending on the change in their porosity, but this method overestimated the average value of the permeability.
4. Li et al. (2005) method gave a valid value of the average permeability of the filter cake and the permeability of each layer can be obtained by combining Li et al. (2005) and Khatib (2004) methods.

References

Al-Abduwani, F.A.H., Bedrikovetsy, P., Farajzadeh, R. et al. 2005. External Filter Cake Erosion: Mathematical Model and Experimental Study. Paper SPE 94635 presented at the European Formation Damage Conference, Sheveningen, The Netherlands, 25-27 May.

Arthur, K.G. and Peden, J.M. 1988. The Evaluation of Drilling Fluid Filter Cake Properties and Their Influence on Fluid Loss. Paper SPE 17617 presented at the International Meeting on Petroleum Engineering, Tianjin, China, 1-4 November.

Civan, F. 1999. Phenomenological Filtration Model for Highly Compressible Filter Cakes Involving Non–Darcy Flow. Paper SPE 52147 presented at the Mid-Continent Operations Symposium, Oklahoma City, Oklahoma, 28-31 March.

Fathi-Najafi, M. and Theliander, H. 1995. Determination of Local Filtration Properties at Constant Pressure. *Separations Technology* **5** (3): 165-178.

Jiao, D. and Sharma, M.M. 1994. Mechanism of Cake Buildup in Crossflow Filtration of Colloidal Suspensions. *Journal of Colloid and Interface Science* **162** (2): 454-462. DOI: DOI: 10.1006/jcis.1060.

Khatib, Z.I. 1994. Prediction of Formation Damage Due to Suspended Solids: Modeling Approach of Filter Cake Buildup in Injectors. Paper SPE 28488 presented at the Annual Technical Conference and Exhibition, New Orleans, Louisiana, 25-28 September.

Lambert, M.E. 1981. A Statistical Study of Reservoir Heterogeneity. MS thesis, The University of Texas at Austin, Austin, Texas, USA (1981).

Li Wenping, C.K., Quintin Richard. 2005. Development of a Filter Cake Permeability Test Methodology. *the American Filtration & Separations Society 2005 International Externalical Conferences & Exposition, September 19-22, Ann Arbor, Michigan* **5**.

Elkatatny, S.M., Mahmoud, M.A., and Nasr-El-Din, H.A. 2011. A New Technique to Characterize Drilling Mud Filter Cake. Paper SPE 144098 presented at the European Formation Damage Conference held in Noordwijk, The Netherlands, 7–10 June.

Theliander, H. and Fathi-Najafi, M. 1996. Simulation of the Build-up of a Filter Cake. *Filtration & Separation* **33** (5): 417-421. DOI: Doi: 10.1016/s0015-1882(97)84302-9.

Tien, C., Bai, R., and Ramarao, B.V. 1997. Analysis of Cake Growth in Cake Filtration: Effect of Fine Particle Retention. *AIChE Journal* **43** (1): 33-44. DOI: 10.1002/aic.690430106.

Tiller, F.M., Lu, R., Kwon, J.H. et al. 1999. Variable Flow Rate in Compactible Filter Cakes. *Water Research* **33** (1): 15-22. DOI: Doi: 10.1016/s0043-1354(98)00192-4.

Zinati, F.F., Farajzadeh, R., Currie, P.K. et al. 2009. Modeling of External Filter Cake Build-up in Radial Geometry. *Petroleum Science and Technology* **27** (7): 746 - 763.

Table 1: Laboratory Formula to Prepare the Equivalent of 1 bbl.

Component	Description/Function	Amount, g
Water	Base liquid	319
Bentonite	Clay for viscosity/API filtrate control	18
Carboxymethylcellulose	API/HP/HT filtrate control	0.25
Highly oxidized leonardite	API/secondary thinner	4.0
Caustic soda	Alkalinity agent	0.6
Calcium carbonate (50 micron)	Weight material/bridging agent	28
Calcium montmorillonite clay	Simulated solids	27

Table 2: Properties of the drilling fluid.

Property		Units	Value
Density		lb/ft^3	69
Plastic Viscosity		cp	12
Yield Point		$lb/100\ ft^2$	8
Gel Strength	@ 10 sec	$lb/100\ ft^2$	4
	@ 10 min		10

*All properties were measured at 120 ^oF, except density which was measured at room temperature.

Table 3: Porosity obtained from the CT scan for external, internal layers and for the ceramic disk.

Filtration Time (min)	External Layer Porosity, vol.%	Internal Layer Porosity, vol.%	Filter Disk Porosity, vol.%
1	85	50	30
3	5	17	30
5	55	45	30
10	20	35	25
15	15	35	25
20	10	30	25
25	5	25	20
30	0	15	20

Table4: Summary of the thickness calculation for the internal and external layers with time.

Filtration Time (min)	External Layer Thickness (in.)	Internal Layer Thickness (in.)	Total cake Thickness (in.)
1	0.04	0.07	0.11
3	0.035	0.06	0.095
5	0.03	0.05	0.08
10	0.06	0.04	0.1
15	0.07	0.05	0.12
20	0.08	0.06	0.14
25	0.085	0.065	0.15
30	0.09	0.07	0.16

Table 5: Changes in filter disk porosity and permeability after filtration process.

Filtration Time (min)	Filter Disk Porosity, vol.%	Final Permeability (md)
1	30	413
3	30	413
5	30	413
10	25	239
15	25	239
20	25	239
25	20	122
30	20	122

Table 6: Average filter cake permeability using Khatib's (1994) method.

Filtration Time (min)	External Layer Porosity, vol.%	Internal Layer Porosity, vol.%	External Layer Permeability (µd)	Internal Layer Permeability (µd)	Average permeability (µd)
1	85	50	30106	1384	2119
3	5	17	26	76	45
5	55	45	2148	891	1142
10	20	35	99	370	140
15	15	35	64	370	97
20	10	30	41	238	63
25	5	25	26	153	41
30	0	15	17	64	25

Table 7: Average filter cake permeability using Li et al.'s (2005) method.

Filtration Time (min)	Filtrate Volume (cm^3)	Filtrate rate ($m^3/m^2.s$)	ΔPm (Pa)	ΔPc (Pa)	Average Cake Permeability K_{ave} (m^2)	Average Cake Permeability K_{ave} (µd)
1	4.42	4.29E-06	13.34	2068414	1.16E-18	1.17
3	4.86	2.38E-06	7.40	2068420	5.54E-19	0.56
5	5.23	1.92E-06	5.97	2068421	3.77E-19	0.38
10	6.10	1.52E-06	8.20	2068419	3.74E-19	0.38
15	6.76	1.30E-06	7.02	2068420	3.84E-19	0.39
20	7.55	1.23E-06	6.64	2068420	4.24E-19	0.43
25	8.06	1.12E-06	6.03	2068421	4.13E-19	0.42
30	8.60	1.05E-06	5.65	2068421	4.13E-19	0.00

Table 8: Calculation of the permeability ratio, pressure drop and the permeability of each layer.

Filtration Time (min)	Permeability Ratio	External Layer Permeability, (µd)	Internal Layer Permeability (µd)	External Layer Pressure drop, (psi)	Internal Layer Pressure drop, (psi)
1	21.76	16.64	0.76	8	292
5	2.41	0.72	0.30	60	240
10	0.27	0.27	1.00	255	45
15	0.17	0.25	1.48	267	33
20	0.17	0.28	1.61	266	34
25	0.17	0.27	1.55	265	35
30	0.27	0.00	1.55	300	0

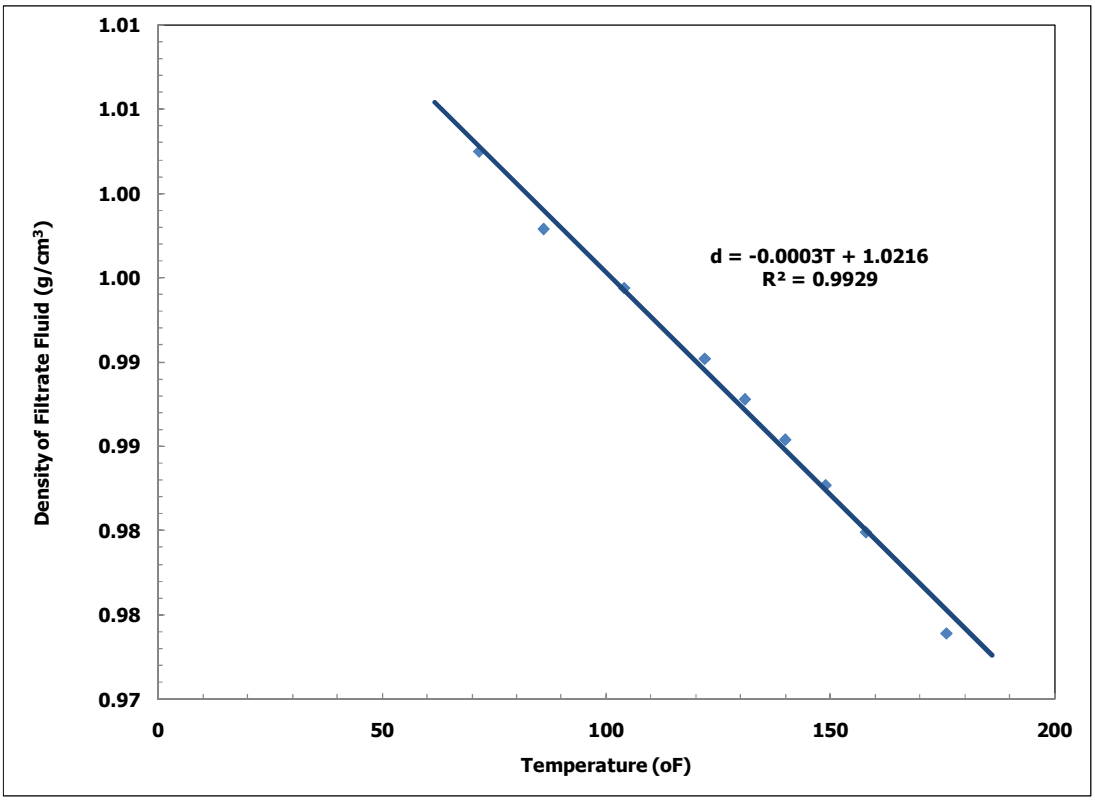

Fig. 1: Change of filtrate fluid density with change in temperature.

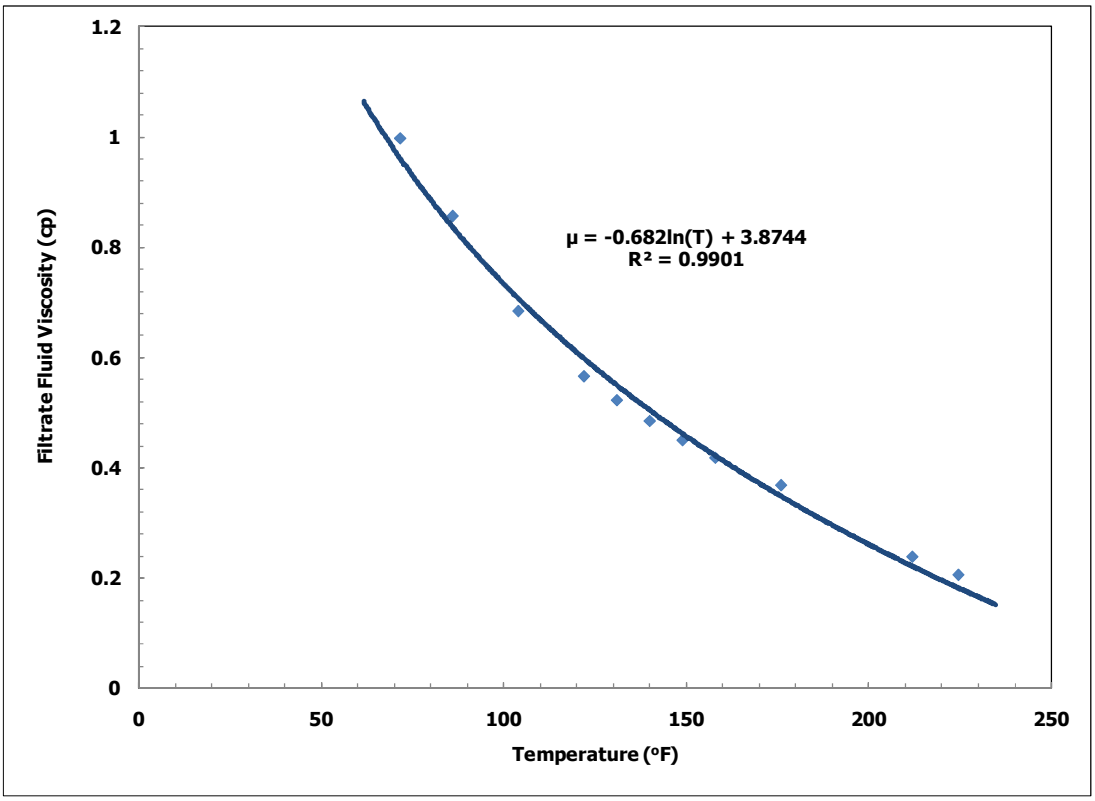

Fig. 2: Change in filtrate fluid viscosity with change in temperature.

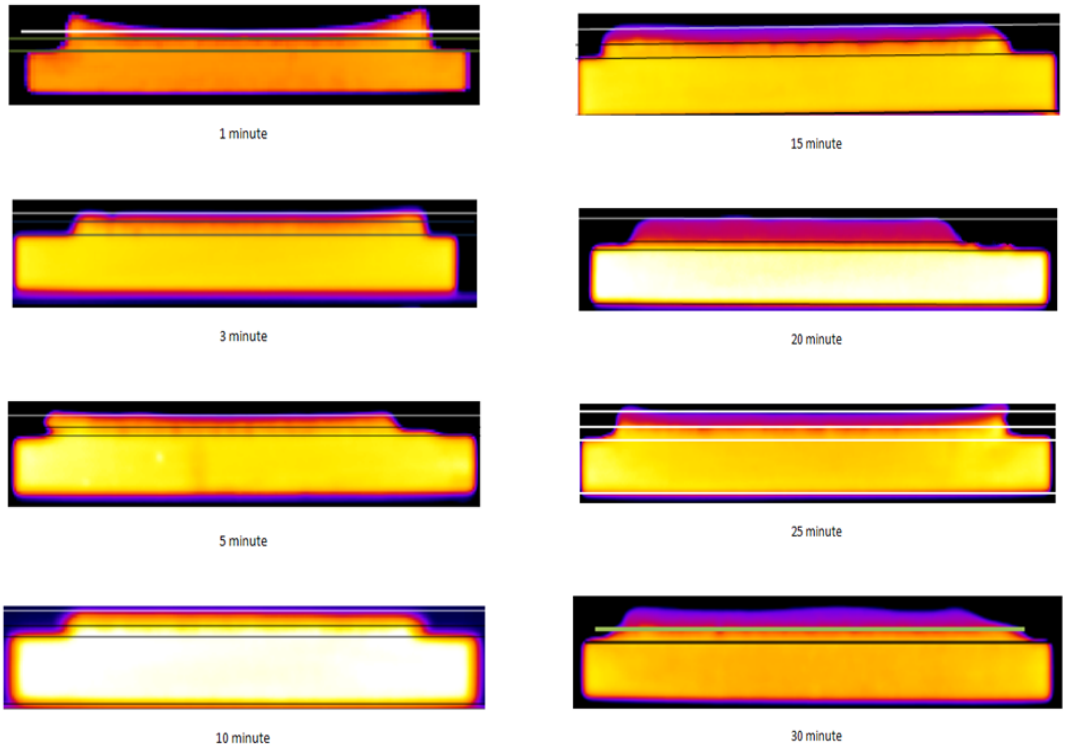

Fig. 3: The CT scanner results for the filter cake at 1, 3, 5, 10, 15, 20, 25, and 30 min. There is a decreasing in thickness from 1 to 5 min for both layers and start of increase after 5 min.

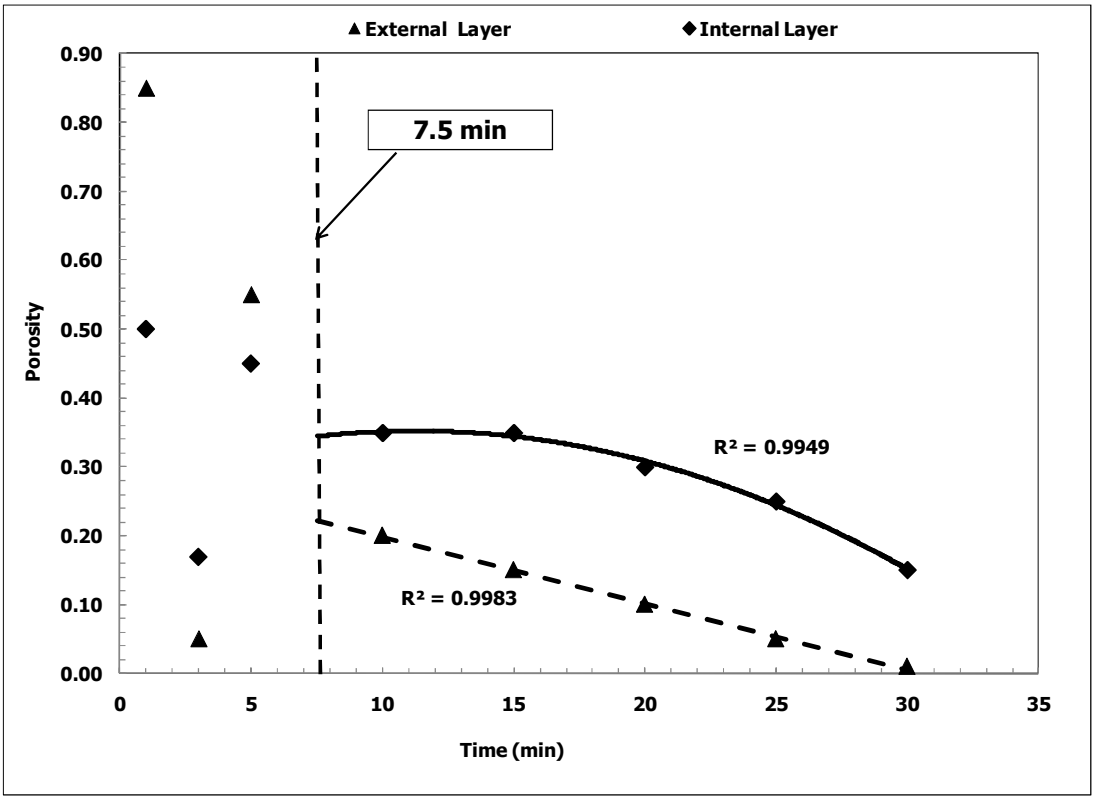

Fig. 4: Change in the average porosity of the internal and external layers. After 7.5 min, there was a logic trend of the porosity for each layer.

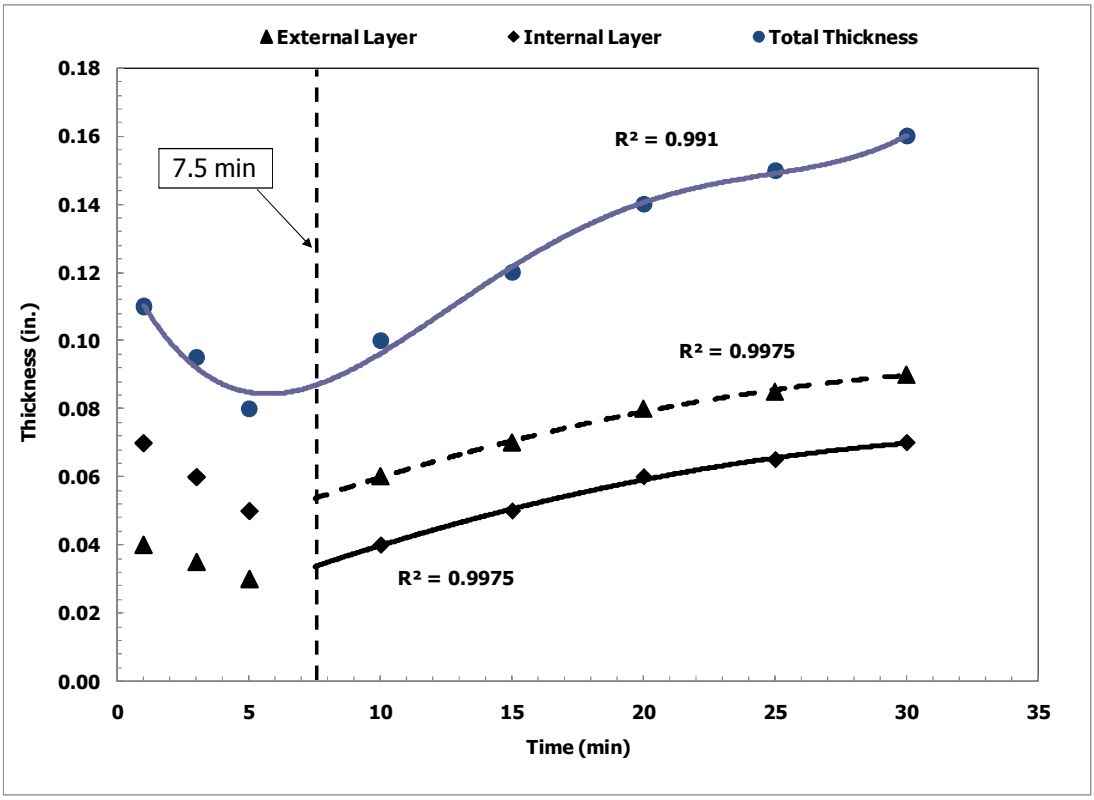

Fig. 5: Change in the thickness of the external and internal layers with time.

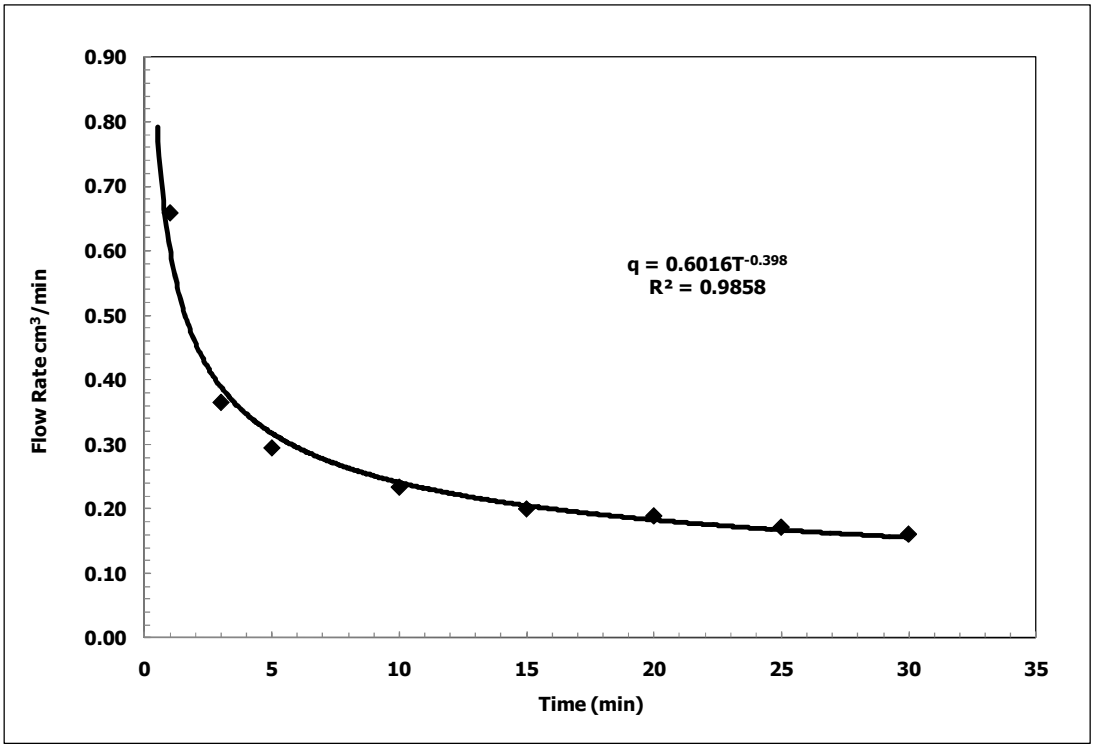

Fig. 6: The reduction of the filtrate rate with time during 30 min of filtration.

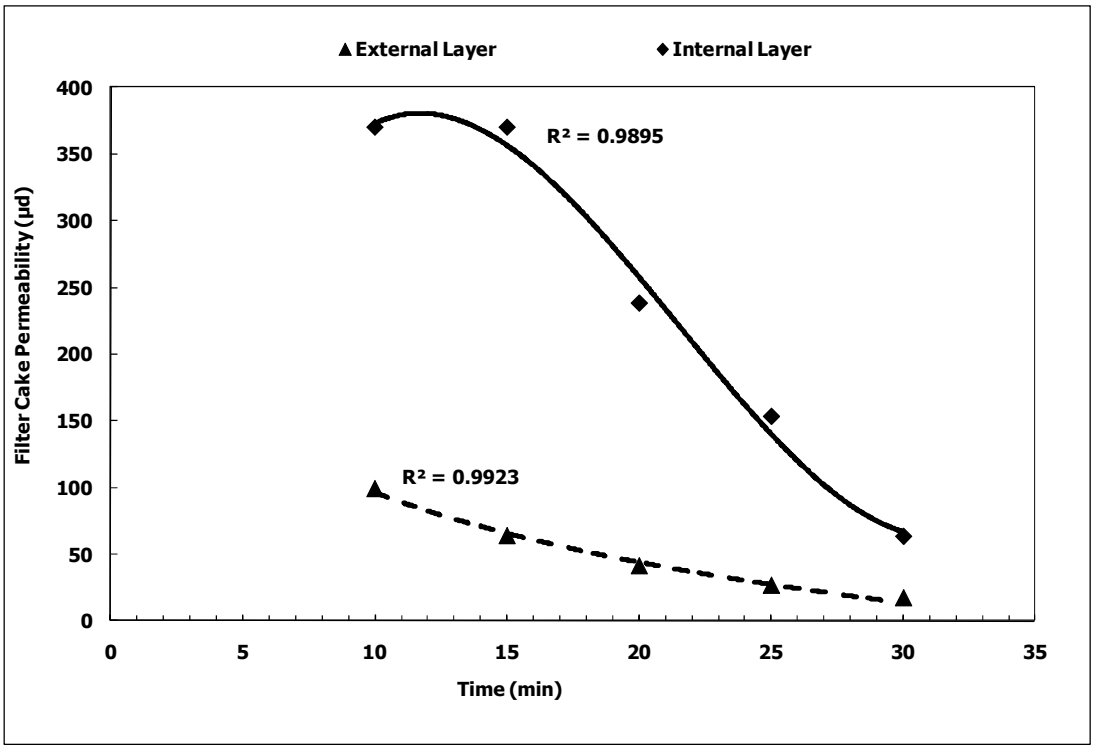

Fig. 7: Average permeability of the external and internal layers calculated using Khatib (1994) model.

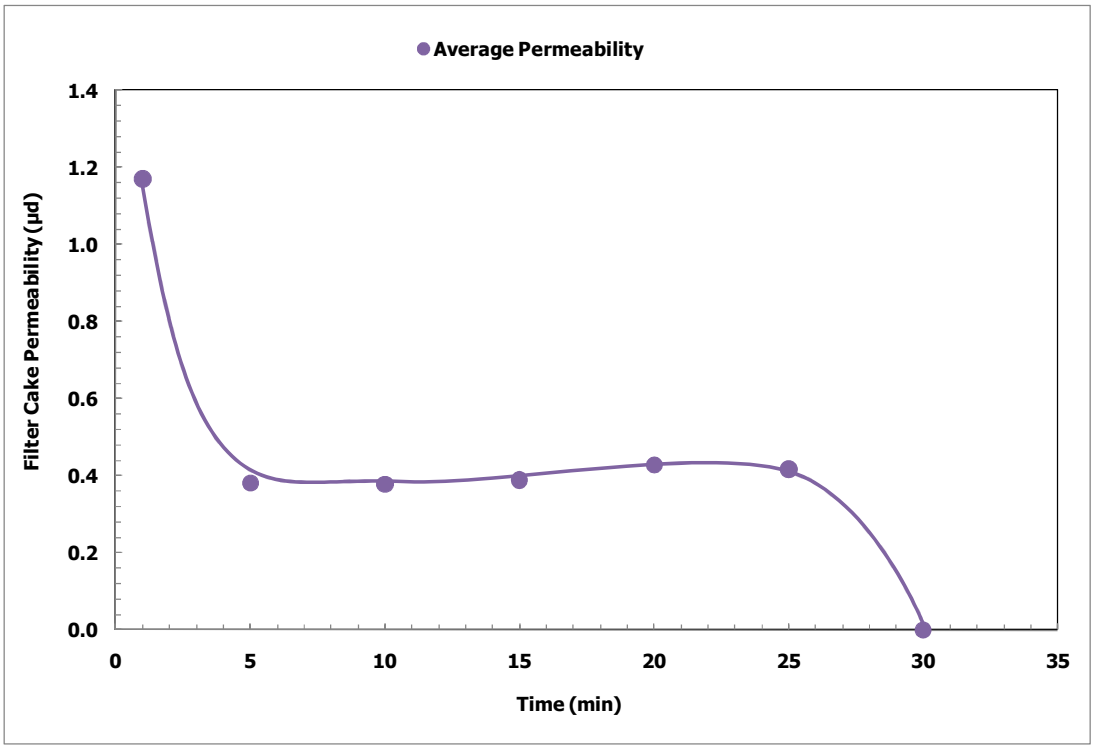

Fig. 8: Average permeability of the filter cake obtained by applying Li et al. (2005) method.

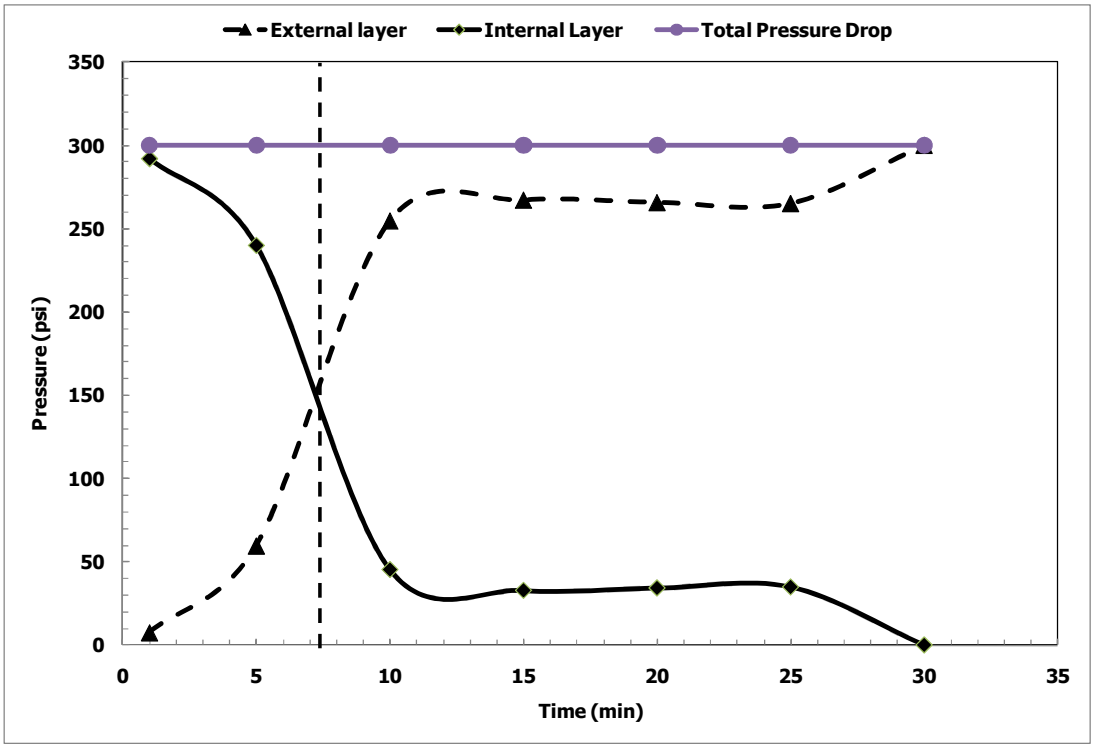

Fig. 9: Pressure drop across the internal and external layer.

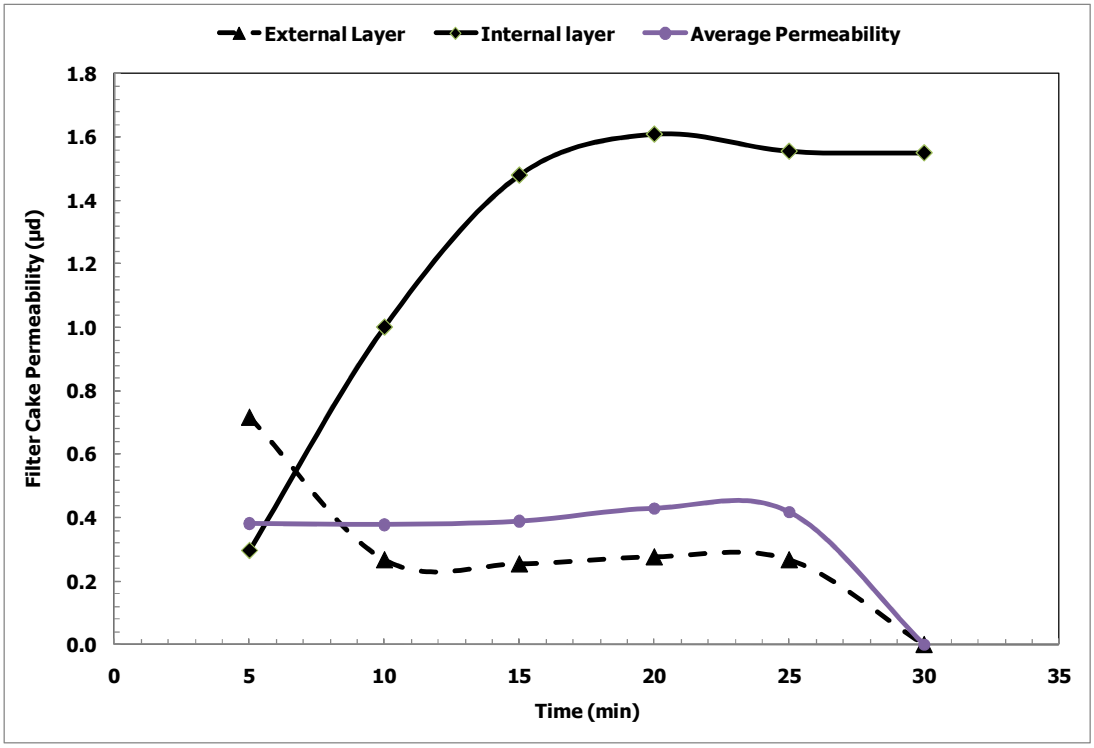

Fig. 10: The permeability of the internal and external layer.